Principy nanomechanické analýzy heterogenních materiálů. Dekonvoluce a homogenizace.

prof. Ing. Jiří Němeček, Ph.D., DSc.

ČVUT Praha, Fakulta stavební

Tvorba výukových materiálů byla podpořena projektem OPVVV, Rozvoj výzkumně orientovaného studijního programu Fyzikální a materiálové inženýrství, CZ.02.2.69/0.0/0.0/16_018/0002274 (2017-18)

EVROPSKÁ UNIE
Evropské strukturální a investiční fondy
Operační program Výzkum, vývoj a vzdělávání

MINISTERSTVO ŠKOLSTVÍ, MLÁDEŽE A TĚLOVÝCHOVY

- **Introduction** and motivation
- Principles of nanomechanical analysis on heterogeneous materials. **Nanoindentation, SEM, image analysis**.
- Nanomechanical analysis of distinct material phases applied to **cement paste, Alkali-activated Fly ash, Gypsum**
- **Up-scaling** phase properties to upper composite level

Introduction

Structural materials are characterized with

- Heterogeneous composition including porosity at different scales *nm-mm*
- **Multi-scale models** must be developed.
- Basic tasks include: **Scale separation**, finding characteristic dimensions (*number of phases, morphology, volumetric content at individual levels)* and **Mechanical characterization** at each scale.

Examples of multi-scale materials

Concrete
4 levels

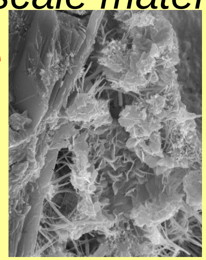

C-S-H gel

Level 1 (~10 nm)

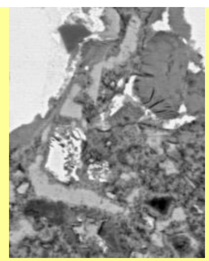

Cement paste (C-S-H, CH, clinker,pores)

Level 2 (~100 um)

Mortar (+sand, Pores, ITZ)

Level 3 (~10 mm)

Concrete (+aggregate, ITZ, pores)

Level 4 (~100 mm)

AAFlyAsh
AAMetakaoline

2 levels

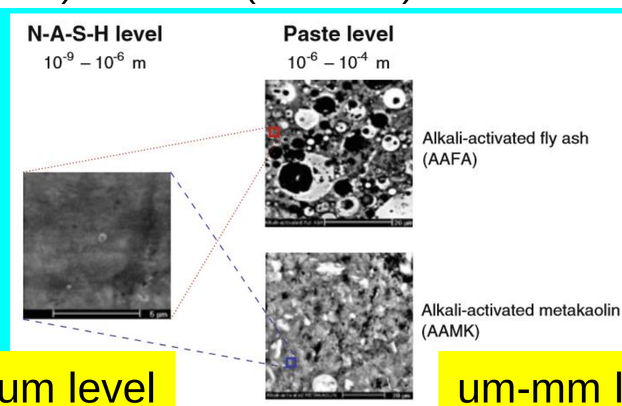

nm-um level

um-mm level

Motivation

Bottom-up approach

¬ Detect and characterize **low-level** material properties.
i.e. Intrinsic (constant) properties of basic building blocks (phases)

¬ Use up-scaling to predict upper-level (**macro/full-scale**) properties knowing volume fractions of phases, microstructural configuration, phase interactions

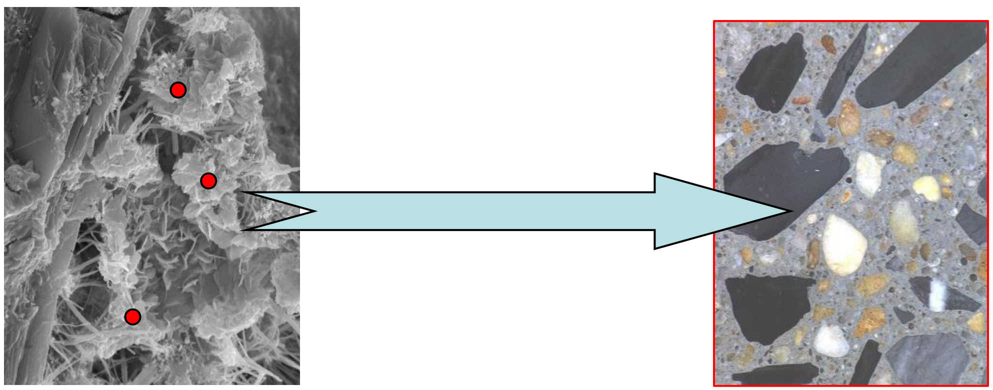

Then, **virtual experiments** are
-possible (changing volume fraction of existing phases, adding new phases)
-less expensive and more predictive than classical macroscopic experiments (one-mixture test)

Available techniques at microscale and their resolution

Microstructural investigations

•**Optical** microscopy: basic morphometrics >>**1 um**

•**SEM:**
SE detector: high resolution on morhology in 2D (100-10.000x)
BSE detector: material constrast
EDX: elemental analysis ~**5 um**

•**AFM** – <u>surface</u> 3D topology (~**1nm**)

•**Micro-CT:** 3D imaging ~**1um**.

•**MIP** porosimetry, pores **nm-um**

Nanomechanical analysis

•**Nanoindentation**
spacial resolution ~**1 um**

•AFM (very local ~**1nm**)

Practical limits:

surface roughness

- unpolished sample ~1-10 um
- polished sample **10-100 nm**

Positioning system – precision

mechanical **~1um**

piezopositioning ~1nm

- pointwise estimates of local mechanical properties
- measurement is performed from the surface but affects volume under the indenter (practically 0.1-1 um³)

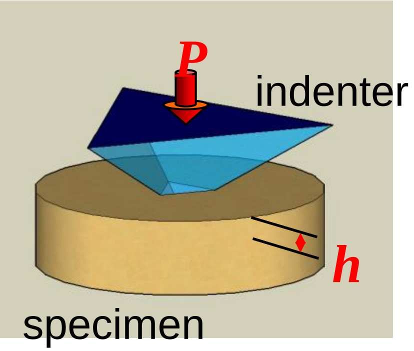

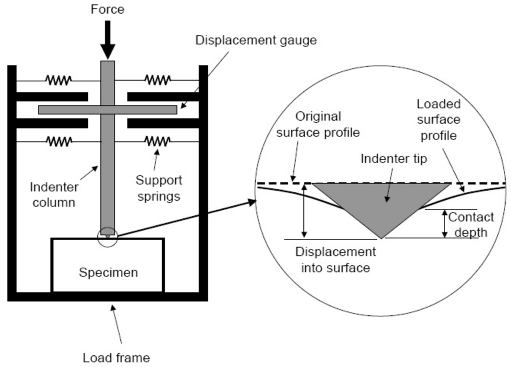

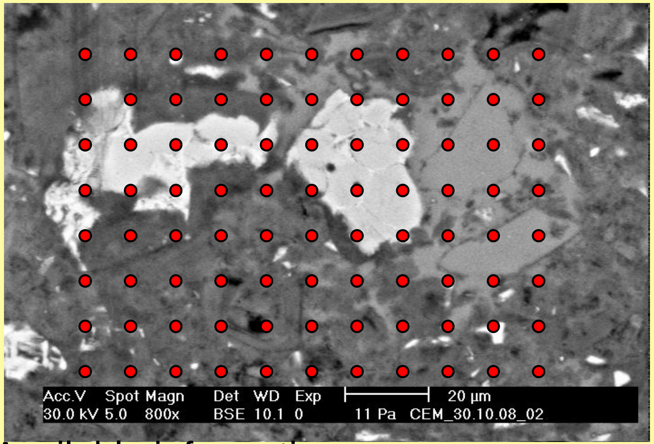

Available information:
Micromechanical characterization
(nanoindentation on phases below 1 um)
Grid nanoindentation, phase deconvolution

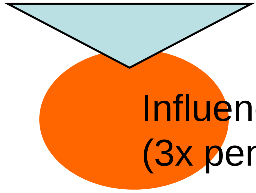

Influence zone, typically 50-500 nm
(3x penetration depth)

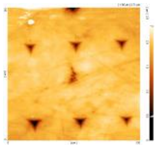

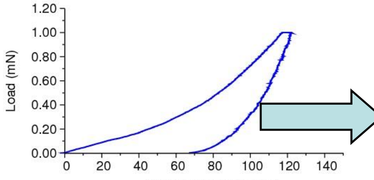

Locally homogenized E, H

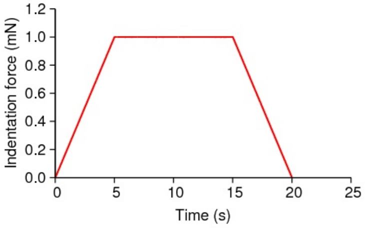

Phase deconvolution in multi-phase systems

Image analysis

Dependent on
-image quality
-pixel luminosity
-segmentation
(thresholds/local minima/
deconvolution of histograms)

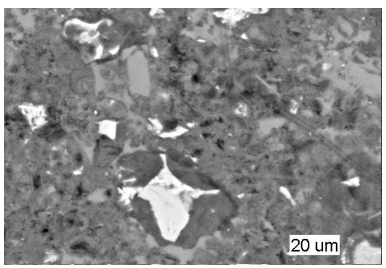

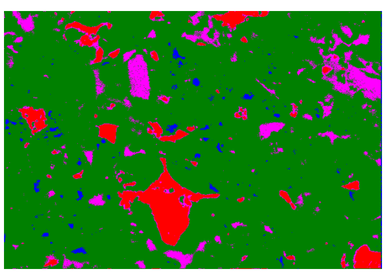

Direct phase deconvolution from mechanical tests -Nanoindentation

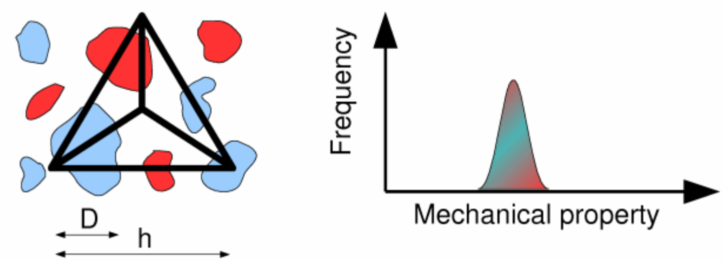

Averaged props.
(h>>D)

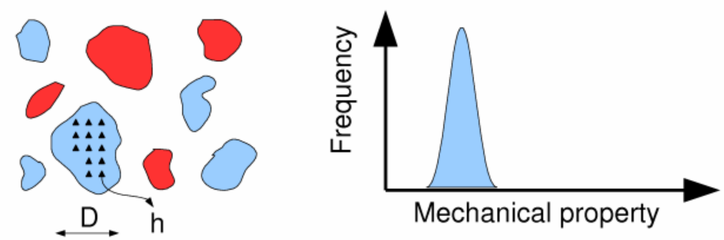

Pointed
(optical image dependent)
(h<<D)

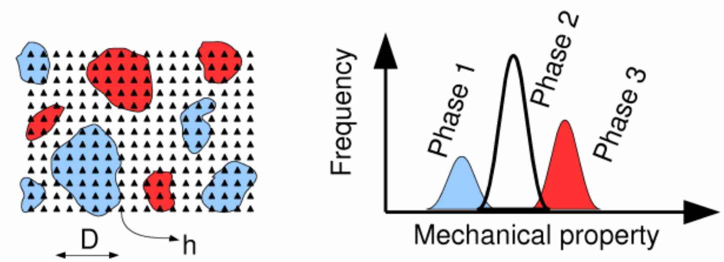

Statistical grid indentation
(h<<D)

Pointed indentation (HD C-S-H)

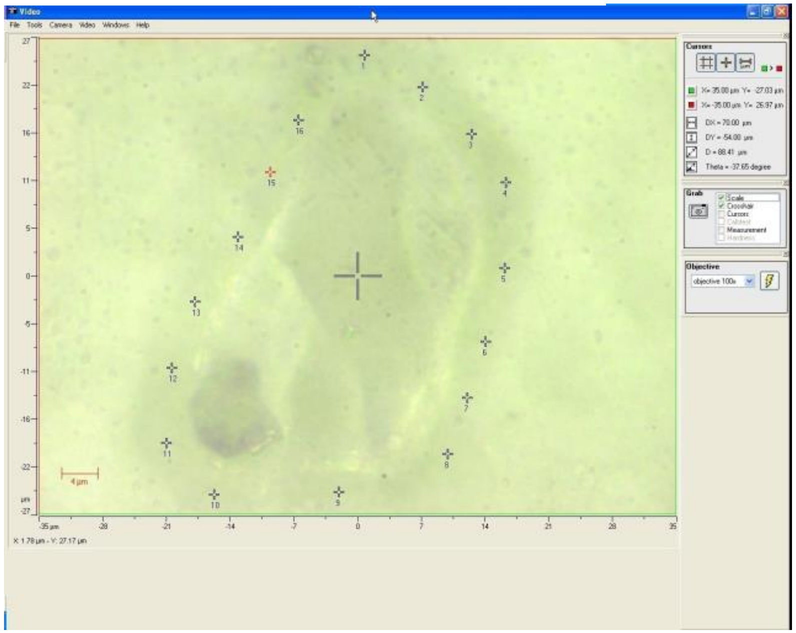

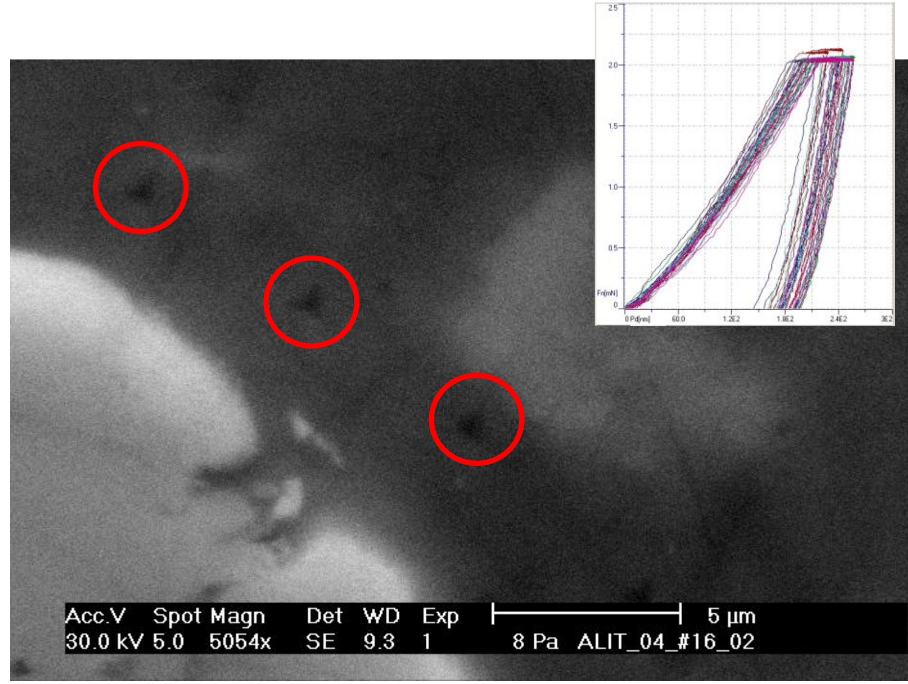

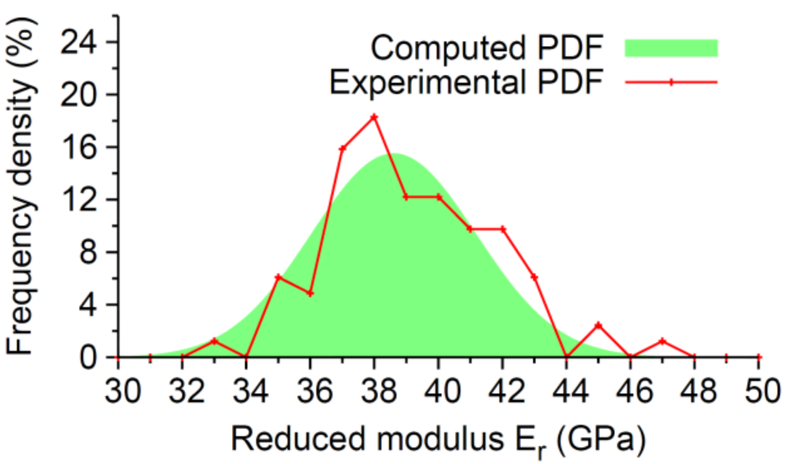

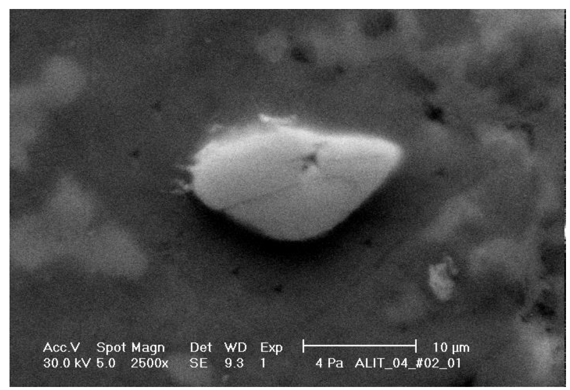

E=38.6± 2.57 GPa

Average properties

Grid indentation –large indents 100mN

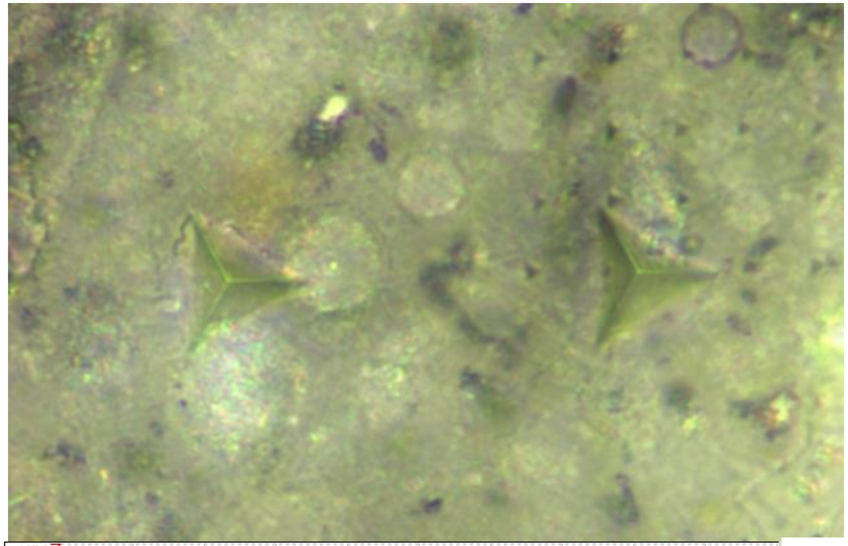

"Physical homogenization"

Geopolymers

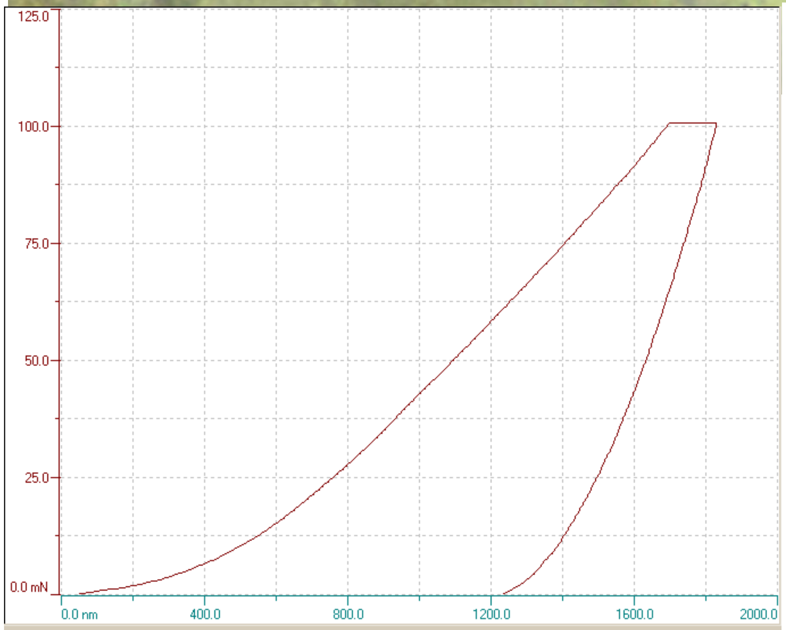

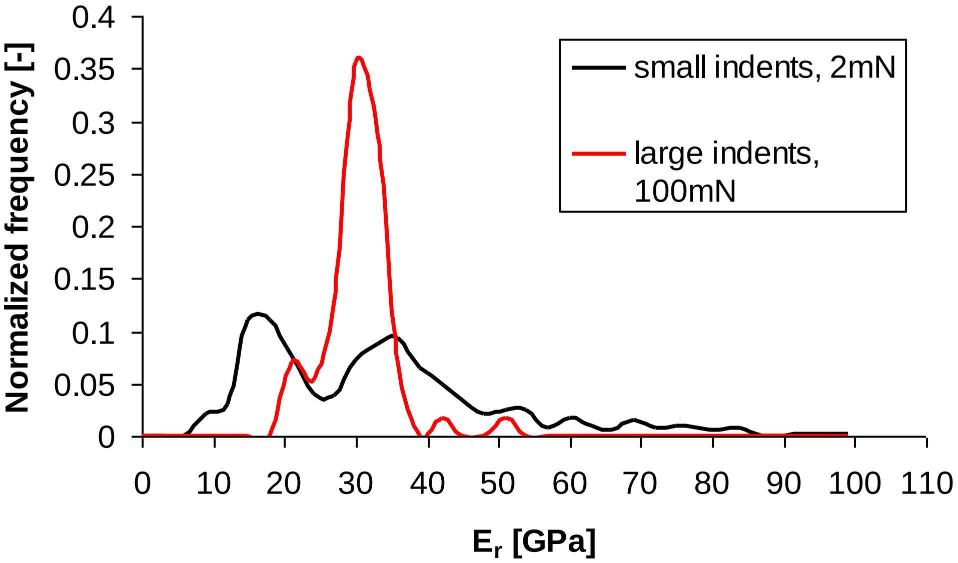

Deconvolution

- All indents taken into account
- Assessment of E modulus from unloading curve (Standard Oliver-Pharr procedure) for individual indents
- Material property can be plotted in the form of property histogram
- Statistical deconvolution of material phases can be applied

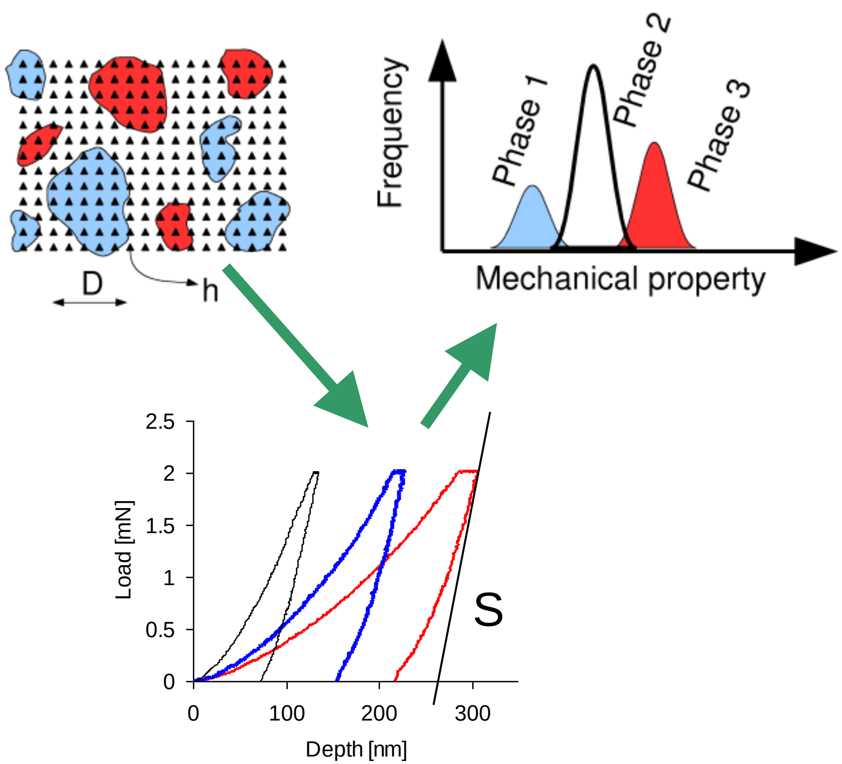

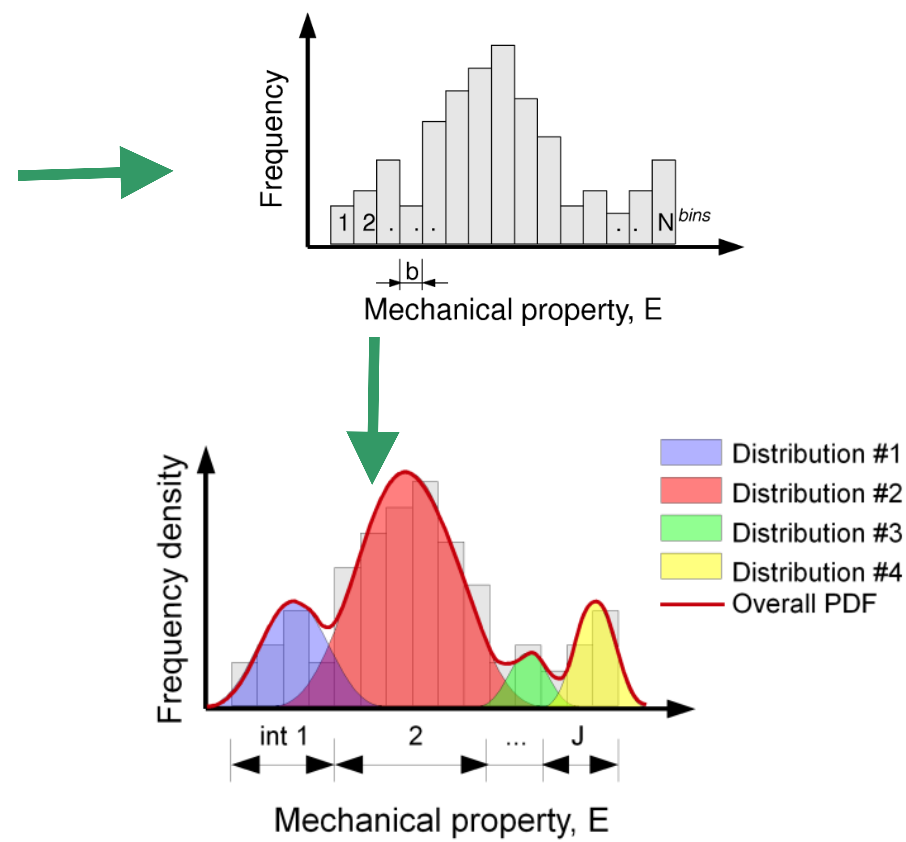

$$E_r = \frac{dP}{dh} \frac{S\sqrt{\pi}}{2\beta\sqrt{A}}$$

Deconvolution algorithm

Ill-posed problem!

Select number of expected phases (e.g. M=2)

$$p_j(x) = \frac{1}{\sqrt{2\pi s_j^2}} exp \frac{-(x-\mu_j)^2}{2s_j^2}$$

Generate M Gauss PDFs (G)

$$\mu_j = \frac{1}{n_j}\sum_{k=1}^{n_j} x_k \qquad s_j^2 = \frac{1}{n_j - 1}\sum_{k=1}^{n_j}(x_k - \mu_j)^2$$

Compute overall theoretical PDF from (G)

$$C(x) = \sum_{j=1}^{M} f_j p_j(x) \qquad f_j = \frac{n_j}{N^{exp}}$$

Compute quadratic norm from deviations between experimental and theoretical PDFs (QN)

$$\boxed{min \sum_{i=1}^{N^{bins}} \left[\left(P_i^{exp} - C(x_i)\right) P_i^{exp}\right]^2}$$

If (QN) < tolerance or max. number of iterations reached

+ Minimum found

\- Next iteration

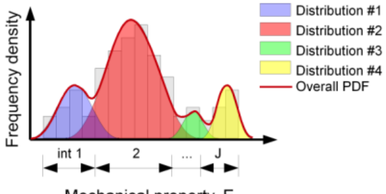

Nanoindentation on cement paste

Main phases at micro-scale

- C-S-H gels (low and high density)
- Portlandite $Ca(OH)_2$
- Residual clinker
- Capillary porosity

Parameters of nanoindentation

- **Representative** material area (*RVE 200x200 um*)
- Indents spacing 10 um
- Individual **indents depth** *h=100-300 nm*

h<< characteristic size of heterogeneities
(Portladite zones, clinker, .. um range)
h>> nanoporosity (30vol.% <100nm) (included in intrinsic phase properties)
h<< Capillary porosity (not included in results)

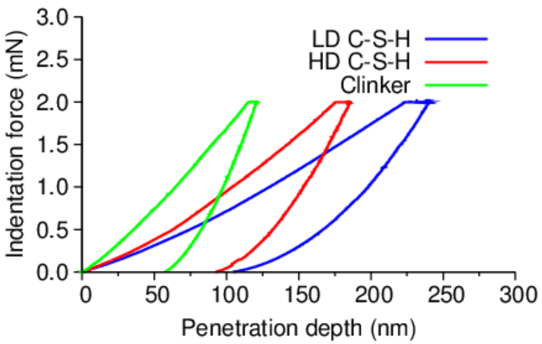

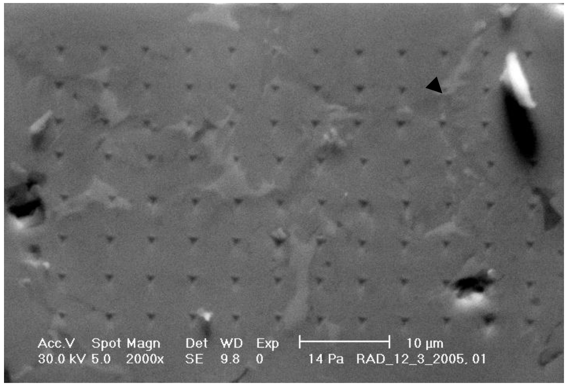

20×20=400 indents
10 µm spacing
RVE size ~200 µm

Nanoporosity included in NI results

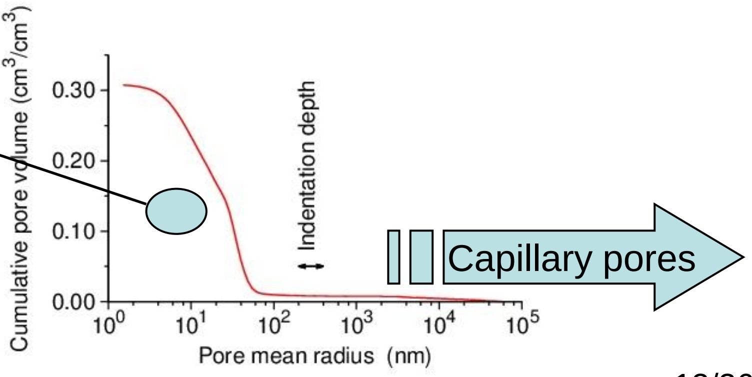

.

- Deconvolution of phases from grid results in RVE

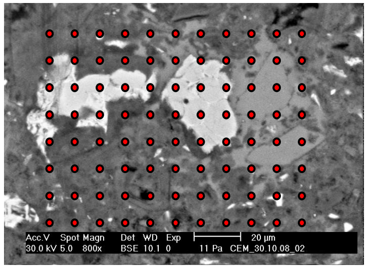

- Assumption of *n*-phases (Gaussian distributions)

$$P(x) = \sum_{j=1}^{n} \frac{p_j}{\sqrt{2\pi s_j^2}} exp\left[-\frac{(x-\mu_j)^2}{2\sigma_j^2}\right]$$

- Minimization of differences between theoretical and experimental probability density

$$\boxed{min \sum_{i=1}^{N^{bins}} \left[\left(P_i^{exp} - C(x_i)\right) P_i^{exp}\right]^2}$$

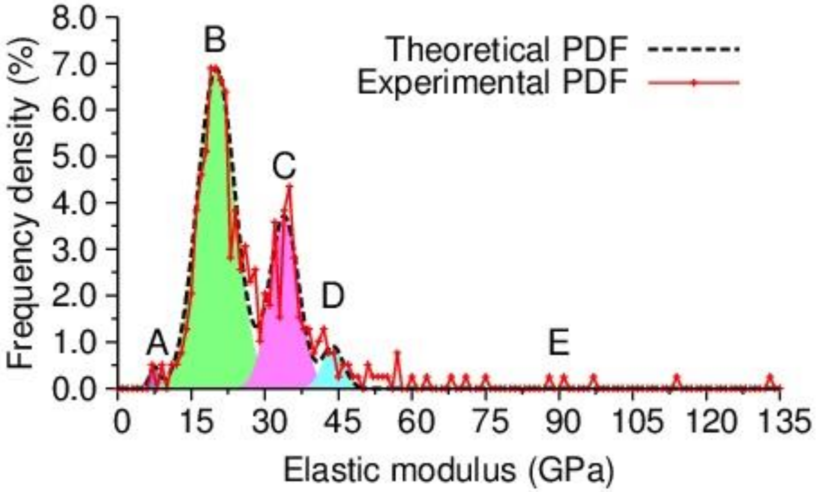

	Reduced modulus E_r (GPa) and frequency of occurance (%)		
Phase	This study[1]	Literature [10] [2]	Literature [22] [3]
A. Low stiffness	**7.45 ± 0.98** (1.05 %)	*n/a*	8.1 ± 1.7 (6 %)
B. LD C-S-H	**20.09 ± 3.85** (63.17 %)	21.7 ± 2.2 (67 %)	18.2 ± 4.19 (51 %)
C. HD C-S-H	**33.93 ± 2.98** (26.34 %)	29.4 ± 2.4 (33 %)	29.1 ± 4.07 (27 %)
D. Portlandite	**43.88 ± 2.15** (4.61 %)	*n/a*	40.3 ± 4.03 (11 %)
E. Non-hydrated	*n/a* (4.83 %)	*n/a*	*n/a*

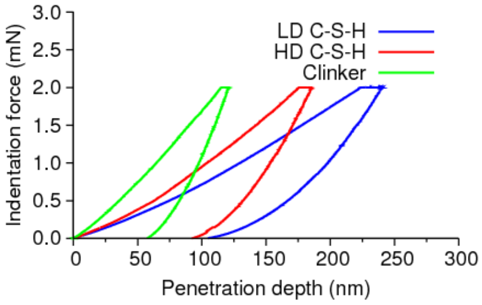

Image analysis (SEM) on cement paste

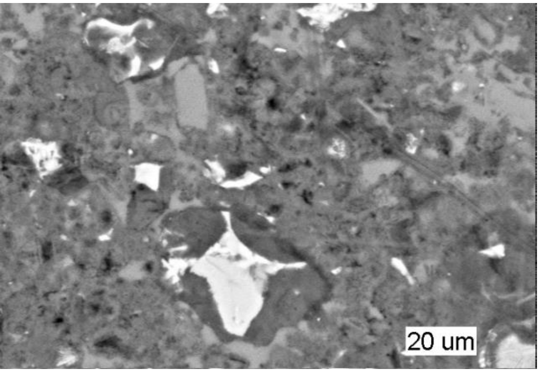

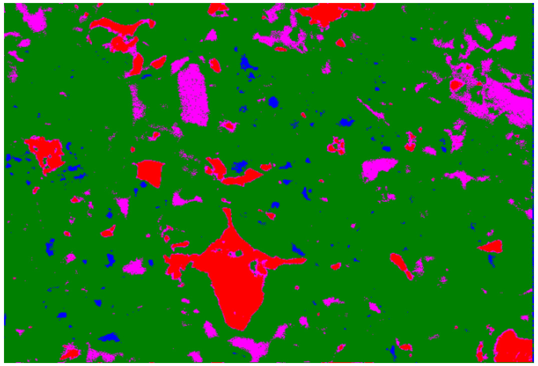

green=C-S-H;
pink=Portlandite;
blue=porosity;
red=clinker

Segmentation

Local minima approach

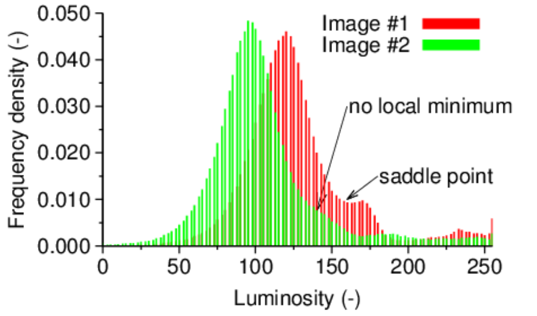

Segmentation to only 4 phases
(Not sufficient contrast to distinguish between low/high-density C-S-H)

Phase	fraction	s.d.
Porosity	**0.017**	0.015
C-S-H	**0.862**	0.024
Portlandite	**0.078**	0.013
Clinker	**0.044**	0.020

Deconvolution approach

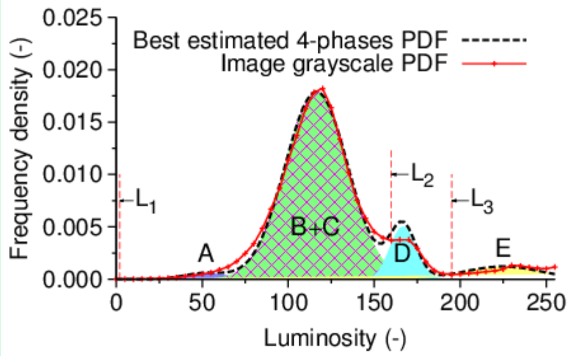

Phase	fraction	s.d.
Porosity	**0.032**	0.02
C-S-H	**0.805**	0.035
Portlandite	**0.101**	0.032
Clinker	**0.062**	0.028

IA insufficiencies

- Cannot sense B/C
- Smooth transitions between phases – no local minima

15/36

Comparison

	Nanoindentation		Image analysis	
Phase	**E (GPa)**	**f_NI**	**f_IA (dec)**	**Error=(f_IA-f_NI)/f_AI**
A-Low stiffness phase	7.45	0.011	0.032	0.66
B=low density C-S-H	20.09	0.632	0.805	-0.11
C=high density C-S-H	33.93	0.263		
D=Portlandite	43.88	0.046	0.101	0.54
E-Clinker	121	0.048	0.062	0.23

- IA overestimates low density regions (pores)
- IA can not sense two types of C-S-H
- IA overestimates Portlandite and clinker volumes (due to smooth color transition)

Nanomechanical analysis of AAFA

Nanomechanical analysis on AAFA

Alkali-activated fly ash (AAFA)

➢Basic reaction product is an amorphous **alumino-silicate gel (N-A-S-H gel) and/or C-S-H gel** forming in the presence of calcium and low alkalinity activator

Nanoindentation

- CSM nanohardness tester
- Several matrices of 10x10=100 imprints
- Mutual indents' spacing 10-50 um
- Total **700 - 800 imprints** per sample
- Load controlled test
- Trapezoidal loading diagram
- Max. load 2 mN
- Loading/holding/unloading 30/30/30s

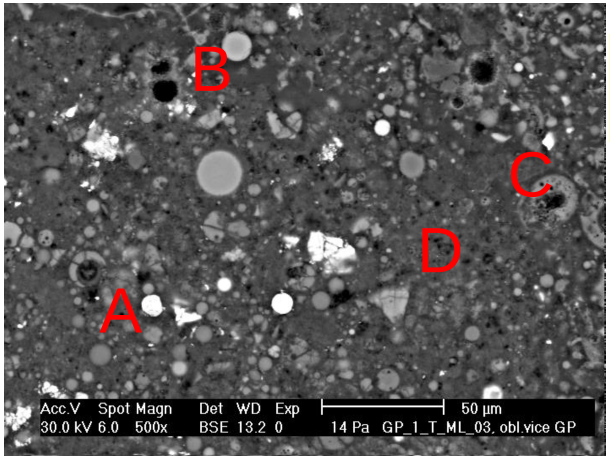

High degree of hetegogeneity

A. light luminous points = iron rich particles (*Fe-Mn* oxides)
B. light grey compact spheres = alumina-silica rich glass particles
C. porous fly ash particles and non-activated slags
D. N-A-S-H gel

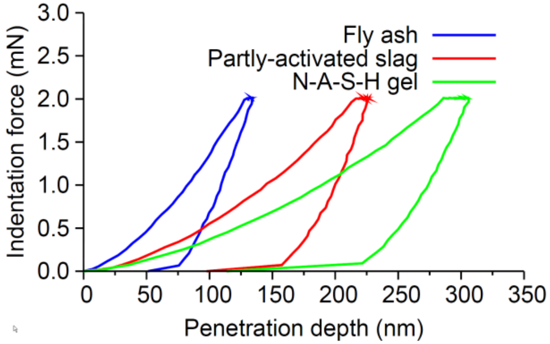

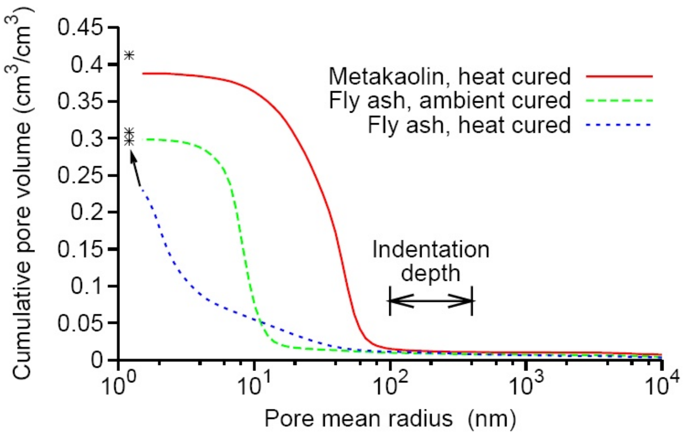

Results on AAFA

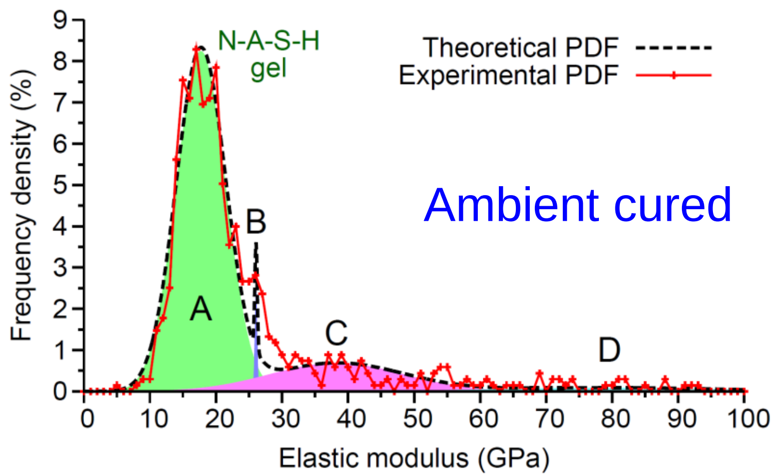

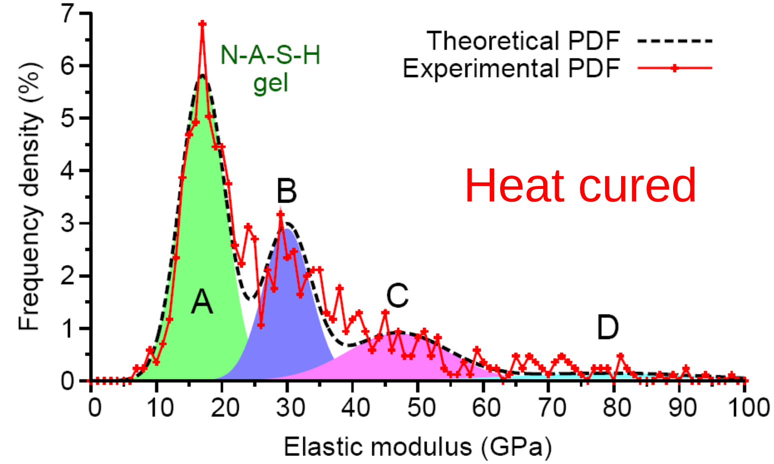

- the second peak comes from partly activated slag particles (mix of gel and rest of a slag particle)
- different reaction kinetics between ambient and heat-cured sample.

Phase / precursor and curing	AAFA Heat-cured	AAFA Ambient-cured
A. N-A-S-H gel	17.03 ± 3.48 (50.7 %)	17.72 ± 3.75 (77.5 %)
B. Partly-activated slag	29.95 ± 3.66 (26.6 %)	26.06 ± 0.18 (1.1 %)
C. Nonactivated slag	46.90 ± 7.76 (17.6 %)	38.27 ± 10.13 (17.5 %)
D. Nonactivated compact glass	79.15 ± 14.34 (5.1 %)	79.65 ± 16.99 (3.9 %)
Unreacted metakaolin		43.91 ± 8.69 (2.8 %)

Phase / precursor and curing	AAMK Heat-cured
A. N-A-S-H gel	17.72 ± 4.43 (97.2 %)
B. Partly-activated slag	-
C. Nonactivated slag	-
D. Nonactivated compact glass	-
Unreacted metakaolin	43.91 ± 8.69 (2.8 %)

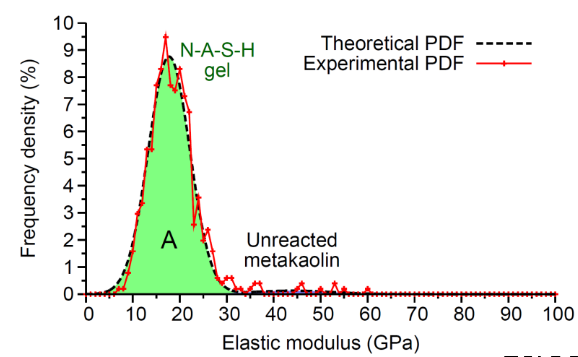

Nanomechanical analysis on gypsum

Nanomechanical analysis on gypsum

Samples:
•low-porosity purified α-hemihydrate ($CaSO_4.1/2H_2O$)
•Used for dental purposes
Microstructure:
•Interlocking crystals+porosity (total 19%)
•The major porosity: in nano-range 0–300 nm (0–100 nm 7%, 100–300 nm 4%, 300–1000 nm 1%)
•virtually no pores appeared between 1-100 μm (<0.5%)

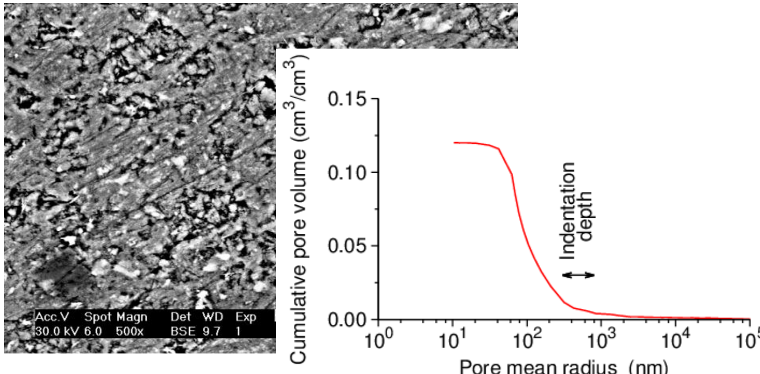

15×12=180 indents
15 μm spacing
RVE size ~200 μm

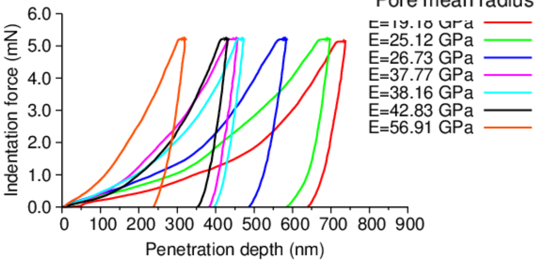

Results:
•polycrystalline nature
•apparent isotropic moduli associated with the indentation volume 1.5^3 $μm^3$ were assessed
•three significant crystallographic orientations (monoclinic system)

3-phases fit

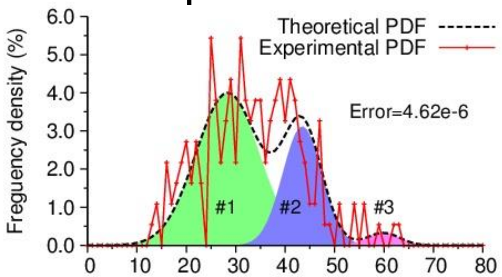

Deconvoluted phase	E (GPa)	Poisson's ratio	Volume fraction
#1	28.36	0.32	0.663
#2	43.46	0.32	0.310
#3	59.89	0.32	0.027

E_{M-T}=32.96 GPa

1-phase fit

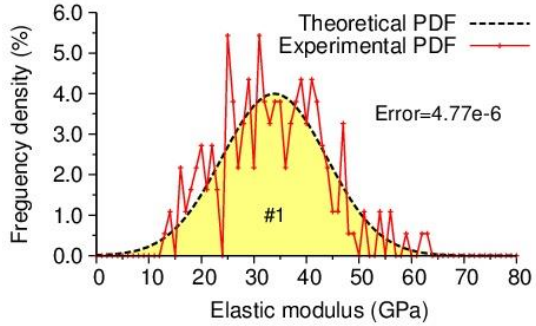

E = 33.90 GPa

Nanomechanical analysis of Al alloy

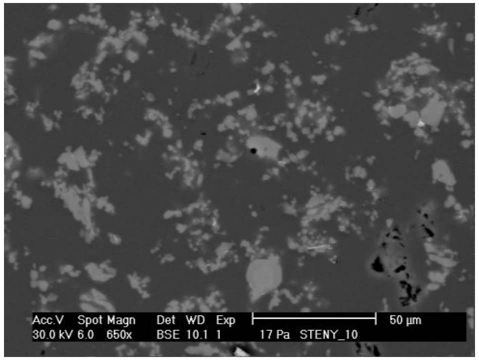

2x(10×10)=2x100 indents
10 µm spacing
RVE size ~100 µm

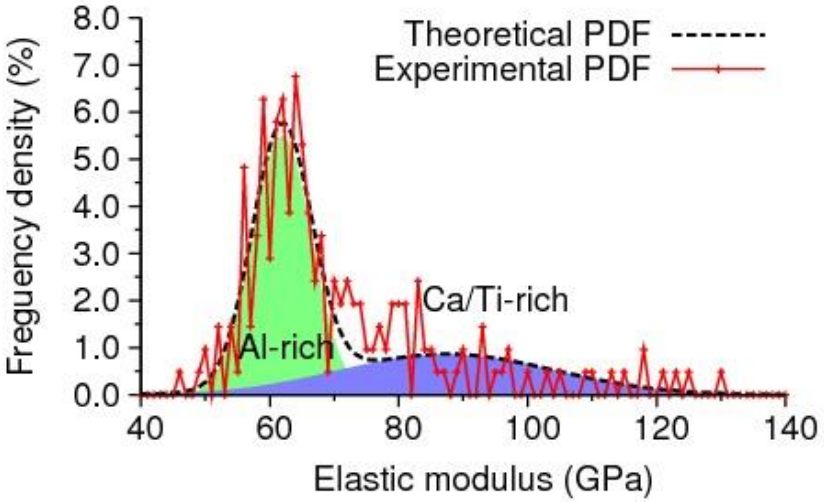

Phase	E (GPa)	Poisson’s ratio (-)	Volume fraction
Al-rich zone	61.882	0.35	0.637681
Ca/Ti-rich zone	87.395	0.35	0.362319

Up-scaling low level properties to upper level

Structural materials (concrete, gypsum, plastics, wood, …) are characterized by

- Multiscale heterogeneity (different chemical and mechanical phases)
- Phase separation process (depends on scale *nm-mm*)

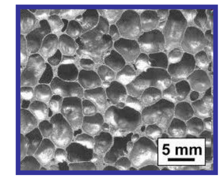

Traditional concept

mm-cm

Overall properties

D

Material = black-box

Micromechanics $d \ll L \ll D$

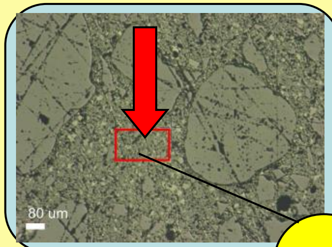

d

Characterization of individual components and microstructure

RVE

L

Effective (homogenized) properties

Microstructure based evaluation

Analytical Upper/Lower Bounds

Voigt bound = strains constant in composite (rule of mixtures for stiffness, parallel configuration)

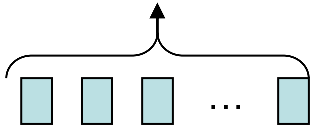

$$E_c = fE_f + (1-f)\,E_m$$

Reuss bound = stresses constant in composite (rule of mixtures for compliance, serial configuration)

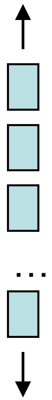

$$E_c = \left(\frac{f}{E_f} + \frac{1-f}{E_m}\right)^{-1}.$$

$$f = \frac{V_f}{V_f + V_m}$$

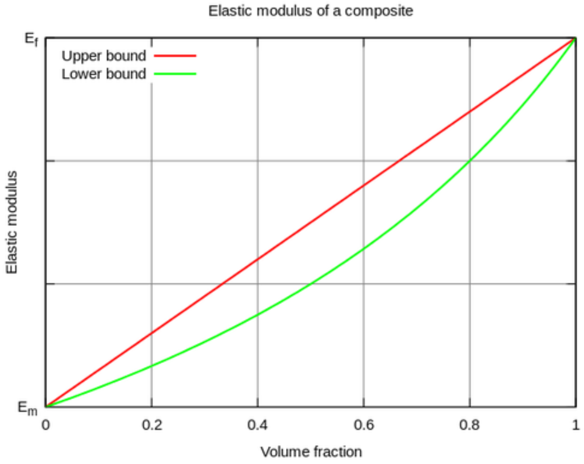

Hashin-Shtrikman Bounds

Micromechanical averaging

1. Analytical schemes

Average stress/strain

$$\langle \boldsymbol{\sigma} \rangle = \frac{1}{V}\int_V \boxed{\boldsymbol{\sigma}(\mathbf{x})}\, dV = \boldsymbol{\Sigma}. \qquad \langle \varepsilon \rangle = \frac{1}{V}\int_V \boxed{\varepsilon(\mathbf{x})}\, dV = \boldsymbol{E}.$$

Local stress

Local strain

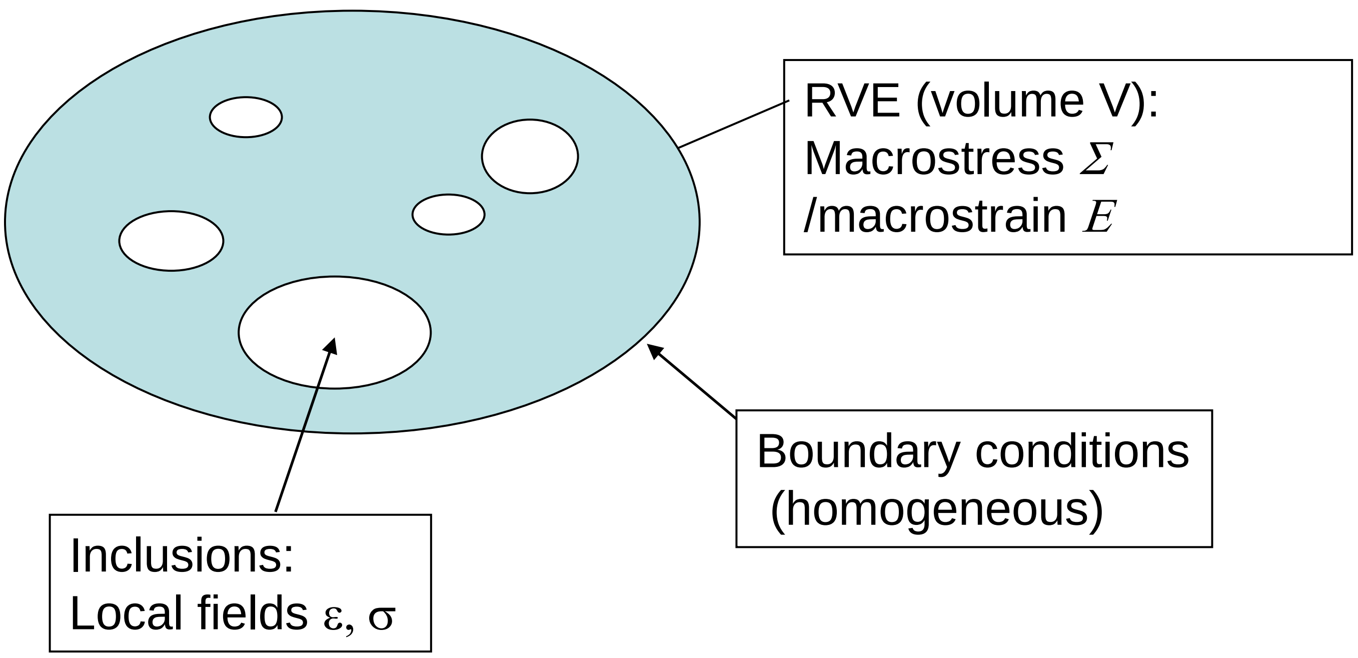

$$\boldsymbol{\Sigma} = \langle \boldsymbol{\sigma} \rangle = \frac{1}{V}\int_V \mathbf{c}(\mathbf{x}) : \mathbf{A}(\mathbf{x}) : \boldsymbol{E}\, dV = \boldsymbol{C}^{\mathit{eff}} : \boldsymbol{E},$$

$$\boldsymbol{E} = \langle \boldsymbol{\varepsilon} \rangle = \frac{1}{V}\int_V \mathbf{s}(\mathbf{x}) : \mathbf{B}(\mathbf{x}) : \boldsymbol{\Sigma}\, dV = \boldsymbol{S}^{\mathit{eff}} : \boldsymbol{\Sigma}.$$

local stiffness and compliance tensors

strain or stress localization (concentration) tensors

For r-phases:

$$\boldsymbol{C}^{\mathit{eff}} = \sum_r f_r \mathbf{c}_r : \mathbf{A}_r$$

$$\boldsymbol{S}^{\mathit{eff}} = \sum_r f_r \mathbf{s}_r : \mathbf{B}_r$$

r-phase medium:
f_r… volume fraction
$\mathbf{c}_r/\mathbf{s}_r$…local stiffness/compliance tensors
$\mathbf{A}_r/\mathbf{B}_r$… localization tensors

Eshelby's estimate

$$\mathbf{A}_r^{est} = \left[\mathbf{I} + \mathbf{S}_r^{Esh} : (\mathbf{C}_0^{-1} : \mathbf{c}_r - \mathbf{I})\right]^{-1} : \left\langle \left[\mathbf{I} + \mathbf{S}_r^{Esh} : (\mathbf{C}_0^{-1} : \mathbf{c}_r - \mathbf{I})\right]^{-1} \right\rangle^{-1}$$

- Based on Eshelby's solution of an ellipsoidal inclusion in an infinite body
- Assumes prevailing matrix reinforced with non-continuous spherical inclusions
- Uses phase volume fractions and stiffnesses (here taken from deconvolution)
- Produces effective (homogenized) composite properties

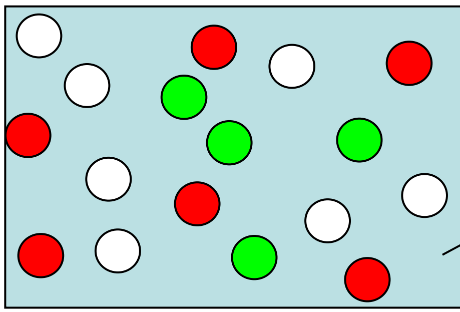

Reference medium == 0-th phase

$$\alpha_0 = \frac{3k_0}{3k_0 + 4\mu_0}, \beta_0 = \frac{6k_0 + 12\mu_0}{15k_0 + 20\mu_0}$$

Bulk and shear effective moduli for r-phase composite:

$$k_{eff} = \frac{\sum_r f_r k_r \left(1 + \alpha_0 \left(\frac{k_r}{k_0} - 1\right)\right)^{-1}}{\sum_r f_r \left(1 + \alpha_0 \left(\frac{k_r}{k_0} - 1\right)\right)^{-1}} \qquad \mu_{eff} = \frac{\sum_r f_r \mu_r \left(1 + \beta_0 \left(\frac{\mu_r}{\mu_0} - 1\right)\right)^{-1}}{\sum_r f_r \left(1 + \beta_0 \left(\frac{\mu_r}{\mu_0} - 1\right)\right)^{-1}}$$

Volume fractions and phase stiffnesses

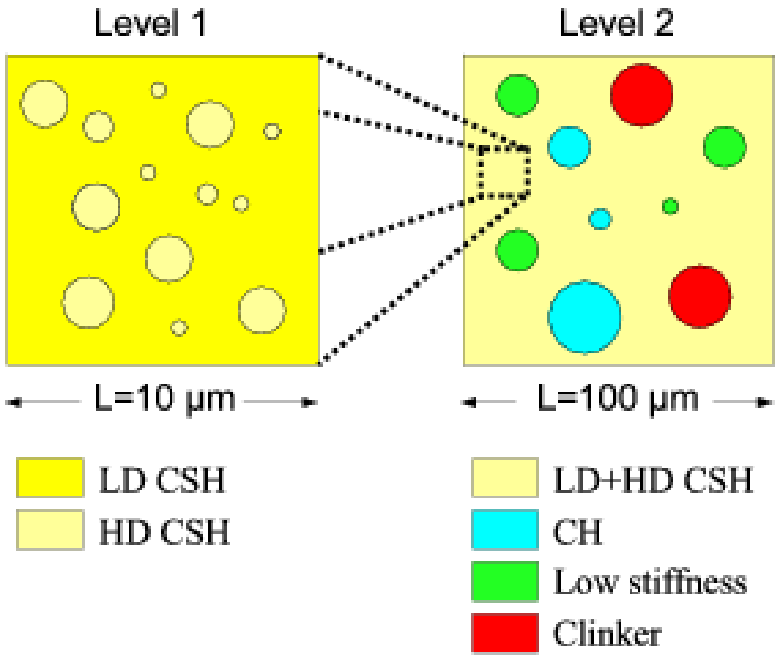

Level 1

	Phase	$E_r(GPa)$	ν	f_r
Input	LD C-S-H	20.09	0.2	0.706
	HD C-S-H	33.93	0.2	0.294
Output	Homogenized C-S-H	**23.363**	0.2	1

Level 2

	Phase	$E_r(GPa)$	ν	f_r
Input	C-S-H	23.363	0.2	0.8951
	Low stiffness	7.45	0.2	0.0105
	CH	43.88	0.3	0.0461
	Clinker	113	0.3	0.0483
Output	Cement paste	**25.343**	0.21	1

FFT based Numerical homogenization

Average strain $\langle \boldsymbol{\varepsilon} \rangle := \frac{1}{|\Omega|}\int_{\Omega} \boldsymbol{\varepsilon}(\mathbf{x})d\mathbf{x} = E$

Governing differential equation:

$$\boldsymbol{\sigma}(\mathbf{x}) = \mathrm{L}(\mathbf{x}) : \boldsymbol{\varepsilon}(\mathbf{x}) \qquad div\boldsymbol{\sigma}(\mathbf{x}) = \mathbf{0} \qquad \mathbf{x} \in \Omega$$

Effective stiffness tensor $\langle \boldsymbol{\sigma} \rangle = \mathrm{L}_{\mathrm{eff}} \langle \boldsymbol{\varepsilon} \rangle$

Decomposition of local strain to *homogeneous strain and polarization part*)

$$\boldsymbol{\varepsilon}(\mathbf{x}) = E - \int_{\Omega} \Gamma^0(\mathbf{x}-\mathbf{y}) : \underbrace{(\mathrm{L}(\mathbf{y}) - \mathrm{L}^0)}_{\text{Polarization stress}} : \boldsymbol{\varepsilon}(\mathbf{y}) d\mathbf{y}$$

(periodic Lippmann-Schwinger integral equation)

Green's operator

Polarization stress

Integral kernel (Green's operator) found in the Fourier space

Discretization (by trigonometric collocation method) leads to
--->nonsymmetric linear system of equations (CG method)

$$[\mathrm{I} + \mathrm{F}^{-1}\hat{\Gamma}\mathrm{F}(\mathrm{L} - \mathrm{L}^0)]\underline{\mathrm{e}} = \mathrm{e}^0$$

Strain at discretization points

Macro strain

Depends only on the stiffness at local grid points

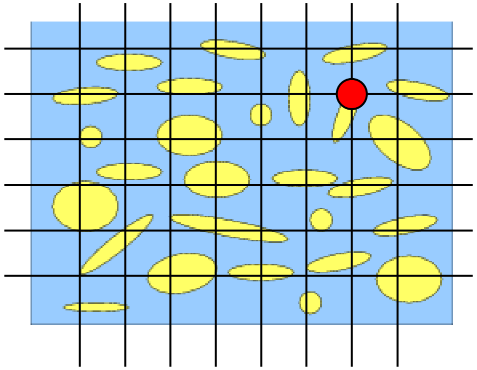

Comparison of the results

Stiffness matrix for **Plane strain** conditions (isotropic material)

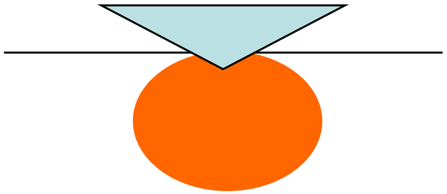

$$\mathbf{L}_{\mathbf{eff}}^{\mathbf{A}} = \frac{E_{eff}}{(1+\nu_{eff})(1-2\nu_{eff})} \begin{bmatrix} 1-\nu_{eff} & \nu & 0 \\ \nu & 1-\nu_{eff} & 0 \\ 0 & 0 & 1-2\nu_{eff} \end{bmatrix}$$

Uni-directional stiffness and Poisson's ratio

Comparison of analytical and FFT scheme

$$\text{stiffness error} = \delta = \sqrt{\frac{\left(\mathbf{L}_{\mathbf{eff}}^{\mathbf{FFT}} - \mathbf{L}_{\mathbf{eff}}^{\mathbf{A}}\right) : \left(\mathbf{L}_{\mathbf{eff}}^{\mathbf{FFT}} - \mathbf{L}_{\mathbf{eff}}^{\mathbf{A}}\right)}{\left(\mathbf{L}_{\mathbf{eff}}^{\mathbf{FFT}} : \mathbf{L}_{\mathbf{eff}}^{\mathbf{FFT}}\right)}}$$

Results from nanoindentation and deconvolution

CEMENT

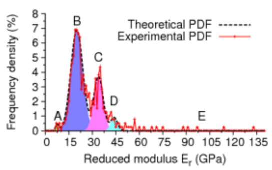

	Phase	E (GPa)	Poisson's ratio (-)	Volume fraction
INPUT	Low stiffness	7.45	0.2	0.0105
	Low density C-S-H	20.09	0.2	0.6317
	High density C-S-H	33.93	0.2	0.2634
	$Ca(OH)_2$	43.88	0.3	0.0461
	clinker	130	0.3	0.0483
OUTPUT	M-T homogenized value	25.3308	0.2067	1.0

GYPSUM

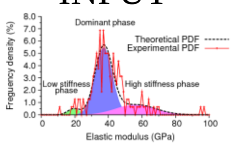

	Phase	E (GPa)	Poisson's ratio (-)	Volume fraction
INPUT	Low stiffness	19.357	0.2	0.043750
	Dominant	37.234	0.2	0.712500
	High stiffness	56.277	0.2	0.243750
OUTPUT	M-T homogenized value	40.000	0.2	1.0

ALPORAS

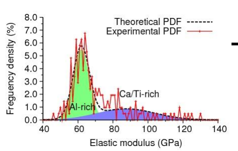

	Phase	E (GPa)	Poisson's ratio (-)	Volume fraction
	Al-rich zone	61.882	0.35	0.637681
	Ca/Ti-rich zone	87.395	0.35	0.362319
OUTPUT	M-T homogenized value	70.083	0.35	1.0

Numerical results

CEMENT

$$\mathbf{L}^{\mathbf{A}}_{\mathbf{eff}} = \begin{bmatrix} 28.145 & 7.036 & 0 \\ 7.036 & 28.145 & 0 \\ 0 & 0 & 21.109 \end{bmatrix} \qquad \mathbf{L}^{\mathbf{FFT}}_{\mathbf{eff}} = \begin{bmatrix} 26.177 & 6.778 & 0.068 \\ 6.778 & 26.224 & 0.014 \\ 0.068 & 0.014 & 19.818 \end{bmatrix}$$

$$^{cement}\delta = 0.071045$$

Error 7.1%

GYPSUM

$$\mathbf{L}^{\mathbf{A}}_{\mathbf{eff}} = \begin{bmatrix} 44.444 & 11.111 & 0 \\ 11.111 & 44.444 & 0 \\ 0 & 0 & 33.333 \end{bmatrix} \qquad \mathbf{L}^{\mathbf{FFT}}_{\mathbf{eff}} = \begin{bmatrix} 40.995 & 10.593 & -0.349 \\ 10.593 & 41.726 & -0.024 \\ -0.349 & -0.024 & 30.909 \end{bmatrix}$$

$$^{gypsum}\delta = 0.075138$$

Error 7.5%

ALPORAS

$$\mathbf{L}^{\mathbf{A}}_{\mathbf{eff}} = \begin{bmatrix} 112.479 & 60.566 & 0 \\ 60.566 & 112.479 & 0 \\ 0 & 0 & 51.913 \end{bmatrix} \qquad \mathbf{L}^{\mathbf{FFT}}_{\mathbf{eff}} = \begin{bmatrix} 117.130 & 62.741 & -0.163 \\ 62.741 & 117.106 & -0.143 \\ -0.163 & -0.143 & 54.313 \end{bmatrix}$$

$$^{Al-alloy}\delta = 0.0393058$$

Error 3.9%

(Stiffness matrices in Mandel’s notation)

Examples of Elastic Homogenization

UHPC

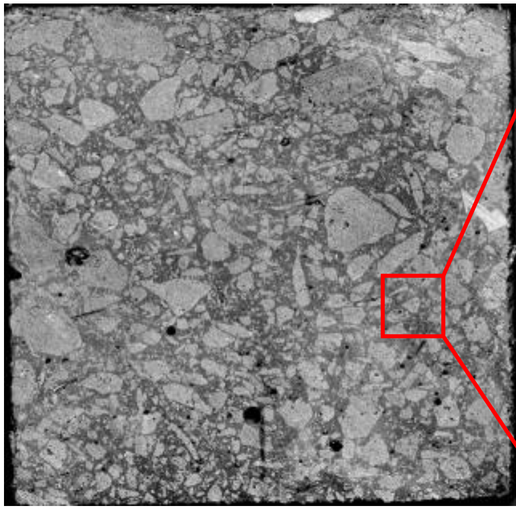

100mm

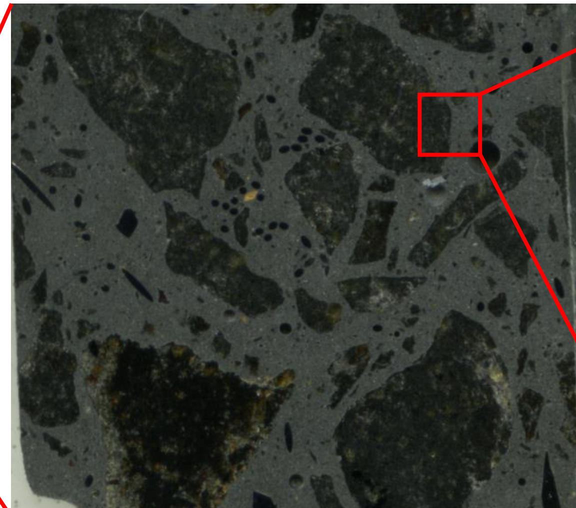

16mm

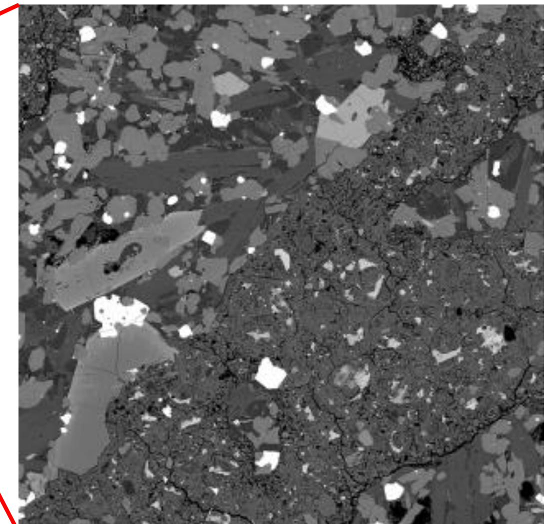

1mm

Level III (matrix+large aggregate)

Main components:
- •Level II
- •Large agg. (21.6%, E=131.1 GPa)
- •pores (2.8%, E=0GPa)

•$E_{eff,\,II}$=55 GPa

Level II (cement matrix+small aggregate+fibers)

Main components:
- •Cement matrix incl. microsilica (58%, E=29.4 GPa)
- •Small agg. 0-4mm (37.5%, E=131.1 GPa)
- •fibers (2%, E=200 GPa)
- •pores (2.8%, E=0GPa)

•$E_{eff,\,II}$=46.6 GPa

Level I (basalt aggregate)

Main components:
- •feldspar (22.8%, E=91 GPa)
- •Olivine (68.4%, E=169 GPa)
- •magnetite (5.2%, E=150 GPa)
- •pores (3.6%, E=0GPa)

•$E_{eff,\,I}$=131.3 GPa

Examples of Elastic Homogenization

Cement paste

Analytical

Data received from statistical deconvolution and homogenized values on cement paste.

Deconvoluted phase	E (GPa)	Poisson's ratio	Volume fraction
Low stiffness phase (A)	7.45	0.2	0.011
Low density C–S–H (B)	20.09	0.2	0.632
High density C–S–H (C)	33.93	0.2	0.263
Portlandite (D)	43.88	0.3	0.046
Clinker (E)	121.0[a]	0.3	0.048
Homogenization			
C–S–H level (B + C) by M–T	23.36	0.2	
C–S–H level (B + C) by SCS	23.41	0.2	
Cement paste level (B + C) + A + D + E by M–T	25.39	0.207	1.0
Cement paste level (B + C) + A + D + E by SCS	25.44	0.208	1.0

from NI

M–T stands for the Mori–Tanaka scheme; SCS stands for the self-consistent scheme.
[a] *Note*: Clinker value was adjusted to 121 GPa according to [7].

$$\mathrm{L}^{\mathrm{A}}_{\mathrm{eff}} = \frac{E_{eff}}{(1+\nu_{eff})(1-2\nu_{eff})}\begin{bmatrix} 1-\nu_{eff} & \nu & 0 \\ \nu & 1-\nu_{eff} & 0 \\ 0 & 0 & 1-2\nu_{eff} \end{bmatrix} = \begin{bmatrix} k+\frac{4}{3}\mu & k-\frac{2}{3}\mu & 0 \\ k-\frac{2}{3}\mu & k+\frac{4}{3}\mu & 0 \\ 0 & 0 & 2\mu \end{bmatrix}$$

$$\text{cement}: L^{A}_{eff} = \begin{bmatrix} 28.44 & 7.43 & 0 \\ 7.43 & 28.44 & 0 \\ 0 & 0 & 21.02 \end{bmatrix}$$

FFT homogenization from NI

$$L^{\mathrm{FFT}}_{eff} = \begin{bmatrix} 26.177 & 6.778 & 0.068 \\ 6.778 & 26.224 & 0.014 \\ 0.068 & 0.014 & 19.818 \end{bmatrix}$$

Comparison

$$\delta = \sqrt{\frac{\left(L^{\mathrm{FFT}}_{eff} - L^{A}_{eff}\right)::\left(L^{\mathrm{FFT}}_{eff} - L^{A}_{eff}\right)}{\left(L^{\mathrm{FFT}}_{eff}::L^{\mathrm{FFT}}_{eff}\right)}}$$

$$^{\text{cement}}\delta = 0.08$$

Gypsum

Analytical

Data received from statistical deconvolution to the three phases and homogenized values on gypsum.

Deconvoluted phase	E (GPa)	Poisson's ratio	Volume fraction
#1	28.36	0.32	0.663
#2	43.46	0.32	0.310
#3	59.89	0.32	0.027
Homogenization method			
M–T	32.96	0.32	1.0
SCS	33.02	0.32	1.0

Note: M–T stands for the Mori–Tanaka scheme; SCS stands for the self-consistent scheme.

$$\text{Gypsum : 3 phase fit : } L_{eff}^{A} = \begin{bmatrix} 47.25 & 22.24 & 0 \\ 22.24 & 47.25 & 0 \\ 0 & 0 & 25.02 \end{bmatrix}$$

$$\text{1phase fit : } L_{eff}^{A} = \begin{bmatrix} 48.51 & 22.84 & 0 \\ 22.84 & 48.51 & 0 \\ 0 & 0 & 25.69 \end{bmatrix}$$

FFT homogenization from NI

$$L_{eff}^{FFT} = \begin{bmatrix} 45.302 & 21.185 & 0.101 \\ 21.185 & 45.497 & -0.008 \\ 0.101 & -0.008 & 24.396 \end{bmatrix}$$

Comparison

$${}^{\text{gypsum}}\delta = 0.07$$